

LETTERS

# Negative lattice expansion from the superconductivity-antiferromagnetism crossover in ruthenium copper oxides

A. C. McLaughlin<sup>1</sup>, F. Sher<sup>2,3</sup> & J. P. Attfield<sup>2</sup>

The mechanism of high-transition-temperature (high- $T_c$ ) superconductivity in doped copper oxides is an enduring problem. Antiferromagnetism is established as the competing order<sup>1,2</sup>, but the relationship between the two states in the intervening 'pseudogap' regime has become a central puzzle<sup>3</sup>. The role of the crystal lattice, which is important in conventional superconductors, also remains unclear. Here we report an anomalous increase of the distance between copper oxide planes on cooling, which results in negative thermal volume expansion, for layered ruthenium copper oxides<sup>4,5</sup> that have been doped to the boundary of antiferromagnetism and superconductivity. We propose that a crossover between these states is driven by spin ordering in the ruthenium oxide layers, revealing a novel mechanism for negative lattice expansion in solids. The differences in volume and lattice strain between the distinct superconducting and antiferromagnetic states can account for the phase segregation phenomena found extensively in low-doped copper oxides, and show that Cooper pair formation is coupled to the lattice. Unusually large variations of resistivity with magnetic field are found in these ruthenium copper oxides at low temperatures through coupling between the ordered Ru and Cu spins.

Layered ruthenium copper oxides are most easily stabilized when the copper oxide planes are in the low doped ('underdoped') superconducting regime. The Ru spins order at 100–140 K, and copper

oxide superconductivity is observed for  $T_c \approx 50$  K (ref. 6). We have investigated how the magnetic order in the RuO<sub>2</sub> layers influences the CuO<sub>2</sub> planes at 5% hole-doping, which is the lower limit for superconductivity in copper oxides. Polycrystalline 1222-type RuSr<sub>2</sub>R<sub>1-x</sub>Ce<sub>0.9</sub>Cu<sub>2</sub>O<sub>10</sub> ceramics (R is a mixture of Nd and other trivalent rare earth elements) were prepared by sintering oxide pellets at 1,000–1,100 °C in air. The pellets are semiconducting down to 4 K, with resistivities at 300 K of 50–100 mΩcm, and do not show superconducting transitions or resistive anomalies at the magnetic transitions described below.

Two spin ordering transitions are observed in magnetoresistance and magnetization measurements on RuSr<sub>2</sub>Nd<sub>0.9</sub>Y<sub>0.1</sub>Ce<sub>0.9</sub>Cu<sub>2</sub>O<sub>10</sub> (Fig. 1a) and are assigned from magnetic neutron scattering (Fig. 2a). Additional neutron diffraction peaks from a (1/2 1/2 1/2) magnetic superstructure appear at temperatures below the Ru spin ordering transition at  $T_{Ru} = 140$  K (Fig. 2a). The magnetic intensities down to 60 K are fitted by a model of antiferromagnetically ordered Ru moments aligned in the *c* direction, as found in the related 1212-type ruthenium copper oxide RuSr<sub>2</sub>GdCu<sub>2</sub>O<sub>8</sub> (ref. 7). (The 1212 materials have only one rare earth layer between ruthenium copper oxide slabs, whereas two layers are present in the 1222 homologues.) The slight canting of Ru moments, which creates a small in-plane ferromagnetism in this and other layered ruthenium copper oxides, is not seen by neutron diffraction but is evidenced in

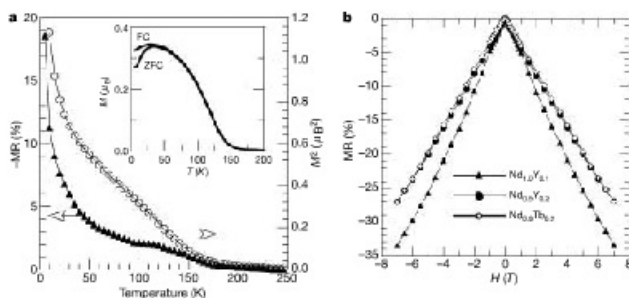


**Figure 1** Magnetization and electronic transport measurements for RuSr<sub>2</sub>R<sub>1-x</sub>Ce<sub>0.9</sub>Cu<sub>2</sub>O<sub>10</sub>. Measurements were made using a 7-T physical properties measurement system. Magnetoresistance, the change of electrical resistance  $\rho$  in applied magnetic field  $H$ , is defined as  $MR_H = (\rho(H) - \rho(0))/\rho(0)$ . **a**, The correlation between negative magnetoresistance ( $-MR$ ) and the square of the magnetization ( $M^2$ ) of RuSr<sub>2</sub>Nd<sub>0.9</sub>Y<sub>0.1</sub>Ce<sub>0.9</sub>Cu<sub>2</sub>O<sub>10</sub> (both measured at  $H = 5$  T), which is typical for ceramic magnetoresistive oxides.  $\mu_B$ , Bohr magneton. The increase in both quantities below 140 K reveals the Ru spin ordering transition ( $T_{Ru}$ ), and the further sharp rises below 60 K coincide with the ordering of Cu spins ( $T_{Cu}$ ). Inset, the divergence of field-cooled (FC) and zero field-cooled (ZFC) magnetizations measured in a low field (0.1 T) also corresponds to  $T_{Cu}$ . The transitions are corroborated by the neutron scattering results in Fig. 2c. **b**, The field dependences of magnetoresistance for several ceramic RuSr<sub>2</sub>R<sub>1-x</sub>Ce<sub>0.9</sub>Cu<sub>2</sub>O<sub>10</sub> samples (key shows R). These are again typical for ceramic spin polarized materials, with a high field  $-|H|$  dependence and additional low field contributions from spin-polarized tunnelling across domain<sup>18</sup> or phase boundaries.

zero field-cooled (ZFC) magnetizations measured in a low field (0.1 T) also corresponds to  $T_{Cu}$ . The transitions are corroborated by the neutron scattering results in Fig. 2c. **b**, The field dependences of magnetoresistance for several ceramic RuSr<sub>2</sub>R<sub>1-x</sub>Ce<sub>0.9</sub>Cu<sub>2</sub>O<sub>10</sub> samples (key shows R). These are again typical for ceramic spin polarized materials, with a high field  $-|H|$  dependence and additional low field contributions from spin-polarized tunnelling across domain<sup>18</sup> or phase boundaries.

<sup>1</sup>Department of Chemistry, University of Aberdeen, Meston Walk, Aberdeen AB24 3UE, UK. <sup>2</sup>Centre for Science at Extreme Conditions and School of Chemistry, University of Edinburgh, King's Buildings, Mayfield Road, Edinburgh EH9 3JZ, UK. <sup>3</sup>Department of Chemistry, University of Cambridge, Lensfield Road, Cambridge CB2 1EW, UK.

magnetization measurements. Below  $T_{Cu} = 60$  K, the Cu spins order antiferromagnetically in the  $a$ - $b$  plane with a  $(1/2, 1/2, 0)$  superstructure—the fitted Ru and Cu spin model is shown in Fig. 2b. Ordering of both Cu and Ru spins has not been previously reported in layered ruthenium copper oxides, and is also surprising because long range Cu spin order persists only up to 2% doping in simple copper oxides such as  $La_{1-x}Sr_xCuO_4$  (although short range antiferromagnetism is observed up to 5% doping). The same two spin ordering transitions are observed by neutron diffraction in  $RuSr_{1-x}Nd_xY_{0.2}Ce_{0.9}Cu_2O_{10}$  and a nominally zero-doped sample,  $RuSr_{1-x}Nd_xY_{0.1}Ce_{0.9}Cu_2O_{10}$ . Both transition temperatures increase with reduced hole-doping, up to  $T_{Ru} = 170$  K and  $T_{Cu} = 120$  K in the latter sample; these and other results are shown in Supplementary Information.

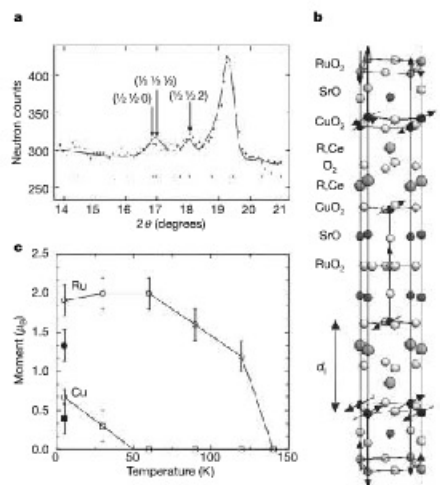


**Figure 2 | Magnetic order in  $RuSr_2Nd_{0.9}Y_{0.2}Ce_{0.9}Cu_2O_{10}$  at low temperatures.** This was determined from high resolution powder neutron diffraction data, collected at a wavelength of 1.5943 Å on instrument SuperD2B at ILL, Grenoble. Magnetic superstructure peaks are labelled on the 4 K diffraction plot (a); the fit is calculated from the refined model for structural and antiferromagnetic Ru and Cu spin ordering (b). The stacking sequence of metal oxide layers and the interplanar separation of copper oxide planes,  $d_i$ , are labelled. Refinement of the tetragonal crystal structure (space group  $I4/mmm$ ) revealed no significant oxygen deficiency (<1%) in the R oxide layers, and the nominal doping level of 0.05 is also corroborated by a bond valence sum calculation using parameters derived previously for layered ruthenium copper oxides<sup>15</sup> which gives an estimate of  $0.06 \pm 0.01$  holes per Cu. These analyses confirm that  $RuSr_2Nd_{0.9}Y_{0.2}Ce_{0.9}Cu_2O_{10}$  is hole-doped to the normal lower limit for superconductivity. c, The temperature variation of the antiferromagnetically ordered Ru and Cu moments (from the slow-cooled experiment described in Fig. 3 legend). Applying a 5-T field at 4 K diminishes the intensities of the antiferromagnetic superstructure peaks (see also Supplementary Information) and the refined moment values (filled symbols in c) are consistent with a  $\sim 45^\circ$  canting of both Ru and Cu moments towards a parallel spin structure. The magnetic alignment axis is unclear from our data but is likely to be in the  $a$ - $b$  plane, as found for  $RuSr_2GdCu_2O_8$  at high field strengths<sup>8</sup>. Error bars, one estimated s.d., calculated from the Rietveld fits to the neutron diffraction profiles.

830

Crystal structure refinements of  $RuSr_2Nd_{0.9}Y_{0.2}Ce_{0.9}Cu_2O_{10}$  from neutron diffraction data show that tetragonal lattice symmetry is preserved down to 4 K, but the cell parameters reveal an unexpected and remarkable change of behaviour at  $T_{Ru}$ . In both slow cooling and slow warming experiments, the unit cell shows a normal (positive) thermal expansion above  $T_{Ru} = 140$  K but below this, the cell shrinks with increasing temperature (Fig. 3a). This negative volume expansion has not been found in other copper oxides (or ruthenium copper oxides) and is unprecedented in magnetic transition metal oxides. No unusual changes in the metal-to-oxygen bond distances are observed, but an anomalous expansion in the separation between copper oxide planes ( $d_i$ ) below  $T_{Ru}$  is seen to drive the negative lattice expansion (Fig. 3b). The negative expansion is not observed when the same sample is quenched to 4 K and then warmed rapidly (Fig. 3a).

Negative expansion at temperatures below an electronic transition results from a crossover between two states of differing volume. In ferromagnets, this is the well-known Invar effect<sup>6</sup>, driven by a crossover from small to large spin states below the Curie transition, for example, in the Invar alloy,  $Fe_{0.64}Ni_{0.36}$ , and in the conducting ferromagnetic oxide  $SrRuO_3$ , although here the volume expansion remains positive below the Curie transition<sup>7</sup>. A distinct, intervalence, mechanism<sup>11</sup> has recently been identified in rare earth compounds such as the fulleride  $Sm_{2.75}C_{60}$  (ref. 11) and  $YbGaGe$  (ref. 12) that change between large, low temperature  $R^{2+}$  and small, high temperature  $R^{3+}$  states. Neither of these mechanisms explains the negative expansion of  $RuSr_2Nd_{0.9}Y_{0.2}Ce_{0.9}Cu_2O_{10}$ , most obviously because the structure, the Ru and Cu valences, and the Ru spin ordering here are not noticeably different to those in previously-characterized superconducting ruthenium copper oxides, none of which show unusual lattice expansion below  $T_{Ru}$  (refs 8, 13, 14). Instead, the proximity of  $RuSr_2Nd_{0.9}Y_{0.2}Ce_{0.9}Cu_2O_{10}$  to the boundary between antiferromagnetism and superconductivity suggests that a crossover between these two states is responsible for the negative expansion. However, as the change from positive to negative expansion occurs at 140 K, well above the possible ordering temperatures for Cu antiferromagnetism or superconductivity, the crossover indicates that two high-temperature correlated states are available for the  $CuO_2$  planes in the pseudogap regime. For convenience, we label these as 'para-antiferromagnetic' and 'parasuperconducting'.

We propose that the 5% doped  $CuO_2$  planes in  $RuSr_2Nd_{0.9}Y_{0.2}Ce_{0.9}Cu_2O_{10}$  are parasuperconducting above 140 K. This precursor state for superconductivity in underdoped copper oxides shows high temperature pairing fluctuations<sup>15</sup> that correspond to pre-formed Cooper pairs in strong coupling theories<sup>16</sup>, but without the phase stiffness between pairs that characterizes the superconducting phase below  $T_c$ . When cooled below 140 K, the Ru spin ordering switches the copper oxide state from parasuperconductivity to para-antiferromagnetism—the state of a paramagnet above a conventional antiferromagnetic transition. Fluctuating clusters of antiparallel copper spins in the para-antiferromagnetic phase condense into the observed long range  $(1/2, 1/2, 0)$  order on cooling to  $T_{Cu} = 60$  K. The switching action of the Ru spin order on the copper oxide planes could be through ferromagnetic pair-breaking from the small in-plane moment, which destabilizes the parasuperconducting state, or through magnetic Ru–Cu exchange, which induces antiferromagnetic Cu spin correlations and so stabilizes para-antiferromagnetism. The latter seems plausible, given the unusual stabilization of long range Cu spin ordering up to 5% doping.

In the above interpretation, the increase in the inter-copper plane distance  $d_i$  below  $T_{Ru}$  (Fig. 3b) shows that the pairing correlations in the parasuperconducting state result in a slight attraction between the copper oxide planes, and the release of this stress below  $T_{Ru}$  drives the negative lattice expansion. This is corroborated by a previous study of a superconducting  $RuSr_2GdCu_2O_8$  sample<sup>17</sup>, in which a small discontinuity in  $d_i$  was found at  $T_{Ru} = 133$  K, although no lattice parameter anomalies or negative expansion resulted. Here, the Ru spin ordering again leads to a slight release of inter-

CuO<sub>2</sub> plane stress, but the pair correlations are stronger in this more highly-doped material so parasuperconductivity survives to low temperatures leading to the zero-resistance state below  $T_c = 35$  K.

The proposed transformation between parasuperconducting and

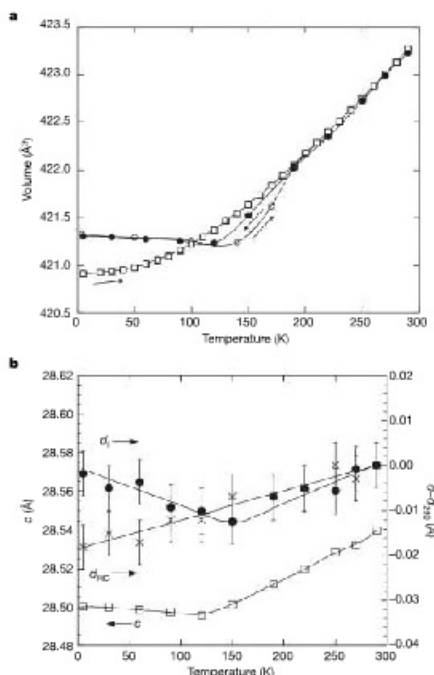


**Figure 3** | Temperature variation of the RuSr<sub>2</sub>Nd<sub>0.9</sub>Y<sub>0.2</sub>Ce<sub>0.9</sub>Cu<sub>2</sub>O<sub>10</sub> structure, revealing negative thermal expansion below the  $T_{Ru} = 140$  K Ru spin ordering temperature. **a**, Volume evolution from three separate powder neutron diffraction experiments on the same sample. 'Slow warming' (open circles; sample was held at 4 K for 5 h then warmed to 290 K at an average rate of 18 K h<sup>-1</sup>) and 'slow cooling' (filled circles; average cooling rate, 16 K h<sup>-1</sup>) data were collected on diffractometer SuperD2B. In the 'fast warming' experiment (open squares) on ILL diffractometer D20 (wavelength 2.42 Å), the sample was quickly cooled to 4 K (at 430 K h<sup>-1</sup>), and diffraction patterns were recorded while warming at 60 K h<sup>-1</sup>. A negative volume expansion is seen below  $T_{Ru}$  in both the slow warming and the slow cooling experiments. The *a* and *c* cell parameters show the same trends as the volumes. The negative volume (*V*) expansion of  $\alpha_V = d(\ln V)/dT = -1.43 \times 10^{-6} \text{ K}^{-1}$  in the 4–140 K interval comes principally from the *c*-axis contribution ( $\alpha_c = -1.39 \times 10^{-6} \text{ K}^{-1}$ ), although the *a* axis also shows a small negative expansion ( $\alpha_a = -0.02 \times 10^{-6} \text{ K}^{-1}$ ). **b**, The *c*-axis length is usefully split into contributions from the thickness of the CuO<sub>2</sub>-SrO<sub>2</sub>-RuO<sub>2</sub>-SrO<sub>2</sub>-CuO<sub>2</sub> ruthenium copper oxide slabs ( $d_{Ru}$ ) and the interplanar separation of copper oxide layers through the (R,Ce)<sub>2</sub>O<sub>2</sub> blocks ( $d_1$ ); marked on Fig. 2b) such that  $c/2 = d_{Ru} + d_1$ . The changes in these distances relative to their 290 K values ( $d_{Ru} = 8.174$ ,  $d_1 = 6.095$  Å) are shown on the right-hand scale of **b**.  $d_{Ru}$  has a monotonic temperature variation, but the separation of the CuO<sub>2</sub> layers  $d_1$  shows an anomalous expansion below  $T_{Ru}$  that mirrors the overall negative expansion of *c*. Error bars, one estimated s.d., calculated from the Rietveld fits to the neutron diffraction profiles.

para-antiferromagnetic states is first order because of the difference in their lattice volumes. This is confirmed by the volume hysteresis in the slow cooling and warming data around  $T_{Ru}$  (Fig. 3a). Furthermore, when the same sample was quenched to 4 K and then warmed rapidly, a low volume state that expands positively up to  $T_{Ru}$  was found, although antiferromagnetic Cu spin ordering was still observed below  $T_{Cu}$  (see Supplementary Figures). This shows that the crossover between parasuperconducting and para-antiferromagnetic spin states occurs rapidly, but the consequent structural relaxation is slower, requiring several hours in our ceramic samples. Similar timescales are observed for low temperature lattice relaxation in phase-separated manganese oxides<sup>18</sup>. From the difference between quenched and slow cooled RuSr<sub>2</sub>Nd<sub>0.9</sub>Y<sub>0.2</sub>Ce<sub>0.9</sub>Cu<sub>2</sub>O<sub>10</sub> lattices, we estimate that the zero temperature superconducting phase has a >0.1% smaller volume and a >0.04% smaller *ca* ratio than the antiferromagnetic phase.

Ru spin ordering in layered ruthenium copper oxides significantly changes the electronic behaviour of low-doped copper oxide planes by extending the limit of long range antiferromagnetic Cu spin order up to the boundary of superconductivity near 5% hole-doping. Another of the consequences of this 'alternative physics' for low-doped copper oxides are large values of negative magnetoresistances (-MR), observed in all of our RuSr<sub>2</sub>R<sub>1-x</sub>Ce<sub>0.9</sub>Cu<sub>2</sub>O<sub>10</sub> samples (Fig 1b). Figure 1a shows that -MR initially rises to ~2% below  $T_{Ru}$ , as is found in superconducting ruthenium copper oxides<sup>19-21</sup>, but increases dramatically on cooling below  $T_{Cu}$ , unlike its behaviour in the superconducting analogues. The -MR<sub>T</sub> = 34% value for RuSr<sub>2</sub>Nd<sub>0.9</sub>Y<sub>0.1</sub>Ce<sub>0.9</sub>Cu<sub>2</sub>O<sub>10</sub> is the largest reported for copper oxides at this field strength. Anisotropic magnetoresistances with -MR<sub>T</sub> up to 20% are found in single crystals of 1% doped antiferromagnetic copper oxides<sup>22,23</sup> (and can increase in higher fields, up to 80% for La<sub>1.99</sub>Sr<sub>0.01</sub>CuO<sub>4</sub> at 14 T). Magnetoresistance results from a field-induced canting of antiferromagnetically-ordered Cu spins towards a parallel alignment in the 1% doped crystals. We find that the Ru spin order in RuSr<sub>2</sub>Nd<sub>0.9</sub>Y<sub>0.2</sub>Ce<sub>0.9</sub>Cu<sub>2</sub>O<sub>10</sub> enhances this effect, as neutron diffraction shows that both Cu and Ru spins are canted towards a parallel alignment by an applied field (Fig. 2c). The large negative magnetoresistance effects observed in our 1222 ruthenium copper oxides are comparable to those in spin-polarized conductors such as colossal magnetoresistance manganese oxide perovskites<sup>24,25</sup> and Sr<sub>2</sub>FeMoO<sub>6</sub> (ref. 26). Phase segregation enhances magnetoresistance in the manganese oxides, and we speculate that parasuperconducting-antiferromagnetic phase coexistence could also contribute to the large magnetoresistance in ruthenium copper oxides.

Our results and our proposed two-state model have several implications for superconductivity in copper oxides. They show that Ru spin ordering creates an alternative physics for low-doped copper oxides that helps to clarify the relationship between antiferromagnetism and superconductivity. The volume difference between the two states demonstrates that Cooper pair formation is coupled to the lattice through a slight attraction between CuO<sub>2</sub> planes, and so a charge-lattice coupling may be necessary for the mechanism of superconductivity. Coupling between carriers and out-of-plane phonons has been demonstrated in recent studies of superconducting bismuth copper oxides<sup>27</sup>. The superconducting and antiferromagnetic correlations are competitive, with different lattice volumes and *ca* ratios for their para-states at a given doping concentration, although the structural transformation between phases is slow. The lattice strains between the two phases may account for the many observations of phase separation, coexistence, and heterogeneities in the pseudogap regime, without requiring electronic segregation into hole-rich and hole-poor regions. A recent theoretical analysis has found that strains resulting from electron-lattice coupling are sufficient to create phase-separated textures over a range of length scales in transition metal oxides<sup>28</sup>.

Finally, we note more general materials science implications. RuSr<sub>2</sub>Nd<sub>0.9</sub>Y<sub>0.2</sub>Ce<sub>0.9</sub>Cu<sub>2</sub>O<sub>10</sub> has revealed a novel mechanism for

negative thermal expansion through a crossover between two different types of antiparallel spin correlation, and other crossovers between competing exotic states may lead to new classes of electronic material showing this useful phenomenon. The ordered Ru spins also enhance spin polarized transport in the doped antiferromagnetic copper oxide planes, leading to magnetoresistances comparable to those of spintronic materials.

Received 10 December 2004; accepted 17 May 2005.

1. Kang, H. J. et al. Antiferromagnetic order as the competing ground state in electron-doped  $\text{Nd}_{1-x}\text{Ce}_x\text{Cu}_2\text{O}_7$ . *Nature* **423**, 522–525 (2003).
2. Hinkov, V. et al. Two-dimensional geometry of spin excitations in the high-temperature superconductor  $\text{YBa}_2\text{Cu}_3\text{O}_{7-x}$ . *Nature* **430**, 650–654 (2004).
3. Orenstein, J. & Mills, A. J. Advances in the physics of high-temperature superconductivity. *Science* **288**, 468–474 (2003).
4. Felner, I., Asaf, U., Levi, Y. & Milo, O. Coexistence of magnetism and superconductivity in  $\text{R}_{1-x}\text{Ce}_x\text{RuSr}_2\text{Cu}_2\text{O}_{7-x}$  ( $\text{R} = \text{Eu}$  and  $\text{Gd}$ ). *Phys. Rev. B* **55**, R3374–R3377 (1997).
5. Noso, C. & Vecchione, A., Cucco, M. & Romano, A. (eds) *Ruthenate and Rutheno-Cuprate Materials* (Springer, Berlin, 2002).
6. Bernhard, C. et al. Coexistence of ferromagnetism and superconductivity in the hybrid ruthenate-cuprate compound  $\text{RuSr}_2\text{GdCu}_2\text{O}_7$ , studied by muon spin rotation and dc magnetization. *Phys. Rev. B* **59**, 14099–14107 (1999).
7. Lynn, J. W., Keimer, B., Ulrich, C., Bernhard, C. & Tallon, J. L. Antiferromagnetic ordering of Ru and Gd in superconducting  $\text{RuSr}_2\text{GdCu}_2\text{O}_7$ . *Phys. Rev. B* **61**, 14964–14967 (2000).
8. van Schilfegaarde, M., Abrikosov, I. A. & Johansson, B. Origin of the Invar effect in iron-nickel alloys. *Nature* **400**, 46–49 (1999).
9. Kiyama, T., Yoshimura, K., Kosuge, K., Ikeda, Y. & Banda, Y. Invar effect of  $\text{SrRuO}_3$ : itinerant electron magnetism of Ru 4d electrons. *Phys. Rev. B* **54**, R756–R759 (1996).
10. Sleight, A. Zero-expansion plan. *Nature* **425**, 674–676 (2003).
11. Avnitiadis, J., Papagelis, K., Margadonna, S., Prassides, K. & Fitch, A. N. Temperature-induced valence transition and associated lattice collapse in samarium fulleride. *Nature* **425**, 599–602 (2003).
12. Salvador, J. R., Guo, F., Hogan, T. & Kanatzidis, M. G. Zero thermal expansion in  $\text{YbGaGe}$  due to an electronic valence transition. *Nature* **425**, 702–705 (2003).
13. McLaughlin, A. C., Attfield, J. P. & Tallon, J. L. A variable temperature structural study of the ferromagnetic superconductor  $\text{RuSr}_2\text{GdCu}_2\text{O}_7$ . *Int. J. Inorg. Mater.* **2**, 95–99 (2000).
14. Shi, L., Li, G., Fan, X. J., Feng, S. J. & Li, X.-G. Structural, transport and magnetic properties of  $\text{RuSr}_2\text{Sm}_{1-x}\text{Ce}_x\text{Cu}_2\text{O}_7$ . *Physica C* **399**, 69–74 (2003).
15. Emery, V. J. & Kivelson, S. A. Importance of phase fluctuations in superconductors with small superfluid density. *Nature* **374**, 434–437 (1995).
16. Yanase, Y. & Yamada, K. Theory of pseudogap phenomena in high- $T_c$  cuprates based on the strong coupling superconductivity. *J. Phys. Soc. Jpn* **68**, 2999–3015 (1999).

17. Chmaissem, O., Jorgensen, J. D., Shaked, H., Dolar, P. & Tallon, J. L. Crystal and magnetic structure of ferromagnetic superconducting  $\text{RuSr}_2\text{GdCu}_2\text{O}_7$ . *Phys. Rev. B* **61**, 6401–6407 (2000).
18. Matsukawa, M. et al. Stretched exponential behaviour in remanent lattice striction of a  $(\text{LaPr})_{1-x}\text{Sr}_x\text{Mn}_2\text{O}_7$  bilayer manganite single crystal. *Phys. Rev. B* **70**, 132402 (2004).
19. Chen, X. H. et al. Transport properties and specific heat of  $\text{RuSr}_2\text{GdCu}_2\text{O}_7$  and  $\text{RuSr}_2\text{Gd}_{1-x}\text{Ce}_x\text{Cu}_2\text{O}_7$  in magnetic fields. *Phys. Rev. B* **63**, 064506 (2001).
20. Awana, V. P. S., Ichihara, S., Karpinen, M. & Yamachi, H. Comparison of magneto-superconductive properties of  $\text{RuSr}_2\text{GdCu}_2\text{O}_7$  and  $\text{RuSr}_2\text{Gd}_{1-x}\text{Ce}_x\text{Cu}_2\text{O}_7$ . *Physica C* **378**, 249–254 (2002).
21. McCrone, J. E. et al. Magnetotransport properties of doped  $\text{RuSr}_2\text{GdCu}_2\text{O}_7$ . *Phys. Rev. B* **68**, 064514 (2003).
22. Ando, Y., Lavrov, A. N. & Komiya, S. Anisotropic magnetoresistance in lightly doped  $\text{La}_{1-x}\text{Sr}_x\text{CuO}_2$ : Impact of antiphase domain boundaries on the electron transport. *Phys. Rev. Lett.* **90**, 247003 (2003).
23. Lavrov, A. N. et al. Spin-flop transition and the anisotropic magnetoresistance of  $\text{Pr}_{1-x}\text{La}_x\text{CeCu}_2\text{O}_7$ : unexpectedly strong spin-charge coupling in the electron-doped cuprates. *Phys. Rev. Lett.* **92**, 227003 (2004).
24. Rao, C. N. R. & Raveau, B. (eds) *Colossal Magnetoresistance, Charge Ordering and Related Properties of Manganese Oxides* (World Scientific, Singapore, 1998).
25. Tokura, Y. (ed.) *Colossal Magnetoresistive Oxides* (Gordon and Breach Science, New York, 2000).
26. Kabaqashi, K. L., Kimura, T., Sawada, H., Terakura, K. & Tokura, Y. Room-temperature magnetoresistance in an oxide material with an ordered double-perovskite structure. *Nature* **395**, 677–680 (1998).
27. Cuk, T. et al. Coupling of the  $B_{1g}$  phonon to the antinodal electronic states of  $\text{Bi}_2\text{Sr}_2\text{Ca}_{1-x}\text{Y}_{1-x}\text{Cu}_3\text{O}_{7-x}$ . *Phys. Rev. Lett.* **93**, 117003 (2004).
28. Ahn, K. H., Lookman, T. & Bishop, A. R. Strain-induced metal-insulator phase coexistence in perovskite manganites. *Nature* **428**, 401–404 (2004).
29. McLaughlin, A. C., Zhou, W., Attfield, J. P., Fitch, A. N. & Tallon, J. L. The structure and microstructure of the ferromagnetic superconductor  $\text{RuSr}_2\text{GdCu}_2\text{O}_7$ . *Phys. Rev. B* **60**, 7512–7516 (1999).
30. McLaughlin, A. C., Attfield, J. P., Asaf, U. & Felner, I. Chemical control of hole-doped superconductivity and magnetism in  $\text{Gd}_{1-x}\text{Ce}_x\text{RuSr}_2\text{Cu}_2\text{O}_7$ . *Phys. Rev. B* **68**, 014503 (2003).

Supplementary Information is linked to the online version of the paper at [www.nature.com/nature](http://www.nature.com/nature).

**Acknowledgements** We thank P. Littlewood, P. Manthou and N. Mathur for discussions, and P. Henry and E. Suard for assistance with the neutron experiments. We also acknowledge the Royal Society of Edinburgh for the SEELLID research fellowship (A.C.M.), the Ministry of Science and Technology, Government of Pakistan for a studentship (F.S.), and the UK EPSRC for beam time provision and financial support.

**Author Information** Reprints and permissions information is available at [www.nature.com/reprintsandpermissions](http://www.nature.com/reprintsandpermissions). The authors declare no competing financial interests. Correspondence and requests for materials should be addressed to J.P.A. (j.p.attfield@ed.ac.uk).